FDTD Analysis of Body-core Temperature Elevation in Children and Adults for Whole-body Exposure

Akimasa Hirata, Takayuki Asano, and Osamu Fujiwara
Department of Computer Science and Engineering, Nagoya Institute of Technology, Japan

E-mail: ahirata@nitech.ac.jp

Abstract

The temperature elevations in anatomically based human phantoms of an adult and a 3-year-old child were calculated for radio-frequency whole-body exposure. Thermoregulation in children, however, has not yet been clarified. In the present study, we developed a computational thermal model of a child that is reasonable for simulating body-core temperature elevation. Comparison of measured and simulated temperatures revealed thermoregulation in children to be similar to that of adults. Based on this finding, we calculated the body-core temperature elevation in a 3-year-old child and an adult for plane-wave exposure at the basic restriction in the international guidelines. The body-core temperature elevation in the 3-year-old child phantom was 0.03°C at a whole-body-averaged specific absorption rate of 0.08 W/kg, which was 35% smaller than in the adult female. This difference is attributed to the child's higher body surface area-to-mass ratio.

1. Introduction

There has been increasing public concern about the adverse health effects of human exposure to electromagnetic (EM) waves. Elevated temperature (1-2°C) resulting from radio frequency (RF) absorption is known to be a dominant cause of adverse health effects, such as heat exhaustion and heat stroke (ACGIH 1996). According to the RF research agenda of the World Health Organization (WHO) (2006), further research on thermal dosimetry of children, along with an appropriate thermoregulatory response, is listed as a high-priority research area.

In the International Commission on Non-Ionizing Radiation Protection (ICNIRP) guidelines (1998), whole-body-averaged specific absorption rate (SAR) is used as a metric of human protection from RF whole-body exposure. In these guidelines, the basic restriction of whole-body-averaged SAR is 0.4 W/kg for occupational exposure and 0.08 W/kg for public exposure. The rationale of this limit is that exposure for less than 30 min. causes a body-core temperature elevation of less than 1°C if whole-body-averaged SAR is less than 4 W/kg (e.g., Chatterjee and Gandhi 1983, Hoque and Gandhi 1988). As such, safety factors of 10 and 50 have been applied to the above values for occupational and public exposures, respectively, to provide adequate human protection.

Thermal dosimetry for RF whole-body exposure in humans has been conducted computationally (Bernardi *et al*. 2003, Foster and Adair 2004, Hirata *et al*. 2007a) and experimentally (Adair *et al*. 1998, Adair *et al*. 1999). In a previous study (Hirata *et al*. 2007a), for an RF exposure of 60 min., the whole-body-averaged SAR required for body-core temperature elevation of 1°C was found to be 4.5 W/kg, even in a man with a low rate of perspiration. Note that the perspiration rate was shown to be a dominant factor influencing the body-core temperature due to RF exposure. The SAR value of 4.5 W/kg corresponds to a safety factor of 11, as compared with the basic restriction in the ICNIRP guidelines, which is close to a safety margin of 10. However, the relationship between the whole-body-averaged SAR and body-core temperature elevation has not yet been investigated in children. The thermoregulatory response in children remains unclear (Tsuzuki *et al.* 1995, McLaren *et al.* 2005). Tsuzuki suggested maturation-related differences in the thermoregulation during heat exposure between young children and mothers. However, for ethical reasons, systemic work on the difference in thermoregulation between young children and adults has not yet been performed, resulting in the lack of a reliable thermal computational model.

In the present study, a thermal computational model of a child was developed parametrically by comparing measured temperatures when exposed to heat in a hot room (Tsuzuki *et al.* 1996, Tsuzuki 1998). At the same time, the effectiveness and limitation of our computational model of the adult is discussed in the same manner. Anatomically based human body phantoms developed by Nagaoka *et al.* (2004, 2005) were used. Using the thermal computation model, we calculated

the SAR and the temperature elevation in adult and child phantoms for plane-wave exposures. Note that EM absorption of the human body at the ICNIRP reference level shows double-hump frequency characteristics. The first peak appears at several dozen megahertz, at which the body resonates electrically, and the second peak, which appears at around 2 GHz, is caused by relaxation of the reference level with the increase in frequency (Dimbylow 2002, Wang *et al.* 2005, Hirata *et al.* 2007a, Conil et al 2008). The discussion in the present paper focuses on the temperature elevation for RF exposures at the resonance frequency of each human phantom and at 2 GHz.

2. Model and Methods

2.1 Human Body Phantoms

Figure 1 illustrates the numeric Japanese female, 3-year-old and 8-month-old child phantoms. The whole-body voxel phantom for the adult female was developed by Nagaoka *et al.* (2004). The resolution of the phantom was 2 mm, and the phantom was segmented into 51 anatomic regions. The 3-year-old child phantom (Nagaoka *et al.* 2005) was developed by applying a free-form deformation algorithm to an adult male phantom (Nagaoka *et al.* 2004). In the deformation, a total of 66 body dimensions was taken into account, and we performed manual editing to maintain anatomical validity. The resolution of these phantoms was kept at 2 mm.

In Section 3.1, we compare the computational results of the present study with the temperatures measured by Tsuzuki (1998). Eight-month-old children were used in her measurements. Thus, we developed an 8-month-old child phantom from a 3-year-old child by linearly scaling using a factor of 0.85 (phantom resolution of 1.7 mm). The height, weight, and surface area of these phantoms are listed in Table 1. The surface area of the phantom was estimated using a formula proposed by Fujimoto and Watanabe (1968).

2. 2. SAR Calculation

The FDTD method (Taflove and Hagness 2003) is used for calculating SAR in the anatomically based human phantom. A vertically polarized plane wave is incident on a human phantom standing in free space. The total-field/scattered-field formulation was applied in order to generate a proper plane wave. To incorporate the anatomically based phantom into the FDTD method, the electrical constants of the tissues are required. These values were taken from the measurements of Gabriel (1996). The computational region has been truncated by applying a twelve-layered perfectly matched layer-absorbing boundary. For harmonically varying fields, the SAR is defined as

$$\mathrm{SAR} = \frac{\sigma}{2\rho}|\mathbf{E}|^2 = \frac{\sigma}{2\rho}(|\hat{E}_x|^2 + |\hat{E}_y|^2 + |\hat{E}_z|^2) \quad (1)$$

where $\hat{E}_x$, $\hat{E}_y$, and $\hat{E}_z$ are the peak values of the electric field components, and σ and ρ are the conductivity and mass density, respectively, of the tissue.

2. 3. Temperature Calculation

The temperature elevation in numeric human phantoms was calculated using the bioheat equation (Pennes 1948). A generalized bioheat equation is given as:

$$C(\mathbf{r})\rho(\mathbf{r})\frac{\partial T(\mathbf{r},t)}{\partial t} = \nabla\cdot(K(\mathbf{r})\nabla T(\mathbf{r},t)) + \rho(\mathbf{r})SAR(\mathbf{r}) + A(\mathbf{r},t) - B(\mathbf{r},t))(T(\mathbf{r},t) - T_B(\mathbf{r},t)) \quad (2)$$

where $T(\mathbf{r},t)$ and $T_B(\mathbf{r},t)$ denote the temperatures of tissue and blood, respectively, C is the specific heat of tissue, K is the thermal conductivity of tissue, A is the basal metabolism per unit volume, and B is a term associated with blood perfusion. The boundary condition between air and tissue for Eq. (2) is expressed as:

$$-K(\mathbf{r})\frac{\partial T(\mathbf{r},t)}{\partial n} = H(\mathbf{r})\cdot(T_s(\mathbf{r},t) - T_e(t)) + SW\left(\mathbf{r}, T_s(\mathbf{r},t)\right) \quad (3)$$

$$SW\left(\mathbf{r}, T_s(\mathbf{r},t)\right) = P_{ins} + SW_{act}\left(\mathbf{r}, T_s(\mathbf{r},t)\right) \quad (4)$$

where H, T_s, and T_e denote, respectively, the heat transfer coefficient, the body surface temperature, and the air temperature. The heat transfer coefficient includes the convective and radiative heat losses. SW is comprised of the heat losses due to perspiration SW_{act} and insensible water loss P_{ins}. T_e is chosen as 28°C, at which thermal equilibrium is obtained in a naked man (Hardy and Du Bois 1938).

In order to take into account the body-core temperature variation in the bioheat equation, it is reasonable to consider the blood temperature as a variable of time $T_B(\mathbf{r},t) = T_B(t)$. Namely, the blood temperature is assumed to be constant over the whole body, since the blood circulates throughout the human body in 1 min. or less (Follow and Neil 1971). The blood temperature variation is changed according to the following equation (Bernardi *et al*. 2003, Hirata *et al*. 2007b):

$$T_B(t) = T_{B0} + \int_t \frac{Q_{BTN}(t)}{C_B\rho_B V_B}\mathrm{d}t \quad (5)$$

where Q_{BTN} is the net rate of heat acquisition of blood from body tissues, C_B (= 4,000 J/kg·°C) is the specific heat, ρ_B (= 1,050 kg/m^3) is the mass density, and V_B is the total volume of blood. V_B is chosen as 700 ml, 1,000 ml, and 5,000 ml for the 8-month-old and 3-year-old child phantoms and the adult phantom (ICRP 1975), respectively.

2. 3. Thermal Constants of Human Tissues

The thermal constants of tissues in the adult were approximately the same as those reported in our previous study (Hirata *et al.* 2006a), as listed in Table 2. These are mainly taken from Cooper and Trezek (1971). The basal metabolism was estimated by assuming it to be proportional to the blood perfusion (Gordon *et al*. 1976), as was the case with Bernardi *et al.* (2003). In the thermally steady state without heat stress, the basal metabolism is 88 W. This value coincides well with that of the average female adult. The basal metabolic rate in the 8-month-old and 3-year-old child phantoms were determined by multiplying the basal metabolic rate of the adult by factors of 1.7 and 1.8, respectively, so that the basal metabolism in these child phantoms coincides with those of average Japanese (Nakayama and Iriki 1987): 47 W and 32 W for 3-year-old and 8-month-old children. Similarly, based on a study by Gordon *et al.* (1976), the same coefficients were multiplied by the blood perfusion rate. The specific heat and thermal conductivity of tissues were assumed to be identical to those of an adult, because the difference in total body water in the child and adult is at most a few percent (ICRP 1975).

The heat transfer coefficient is defined as the summation of heat convection and radiation. The heat transfer coefficient between skin and air and that between organs and internal air are denoted as H_1 and H_2, respectively. Without heat stress, the following equation is maintained:

$$\int_v A(\mathbf{r})dv = \int_S P_{ins}(\mathbf{r})dS + \int_S H(\mathbf{r},t)(T(\mathbf{r},t) - T_a)dS \qquad (6)$$

where T_a is the air temperature. The air temperature was divided into the average room temperature T_{a1} (28°C) and the average body-core temperature T_{a2}, corresponding to H_1 and H_2, respectively.

Insensible water loss is known to be roughly proportional to the basal metabolic rate: 20 ml/kg/day for an adult, 40 ml/kg/day for a 3-year-old child, and 50 ml/kg/day for an 8-month-old child (Margaret *et al*. 1942). For the weight listed in Table 1, the insensible water losses in the phantoms of a female adult, a 3-year-old child, and an 8-month-old child are 29 W, 15.3 W, and 12.7 W, respectively. Note that the insensible water loss consists of the loss from skin (70%) and the loss from the lungs through breathing (30%) (Karshlake 1972). The heat loss from the skin to the air P_{ins1} and that from the body-core and internal air P_{ins2} are calculated as listed in Table 3.

For the human body, 80% of the total heat loss is from the skin and 20% is from the internal organs (Nakayama and Iriki 1987). Thus, the heat loss from the skin is 68 W in the adult female, 37.6 W in the 3-year-old child, and 25.6 W in the 8-month-old child. Similarly, the heat loss from the internal organs is 17 W in the adult female, 9.4 W in the 3-year-old child, and 6.4 W in the 8-month-old child. Based on the differences among these values and the insensible water loss presented above, we can obtain the heat transfer coefficients, as listed in Table 3.

In order to validate the thermal parameters listed in Table 3, let us compare the heat transfer

coefficients between skin and air obtained in the present study to those reported by Fiala *et al.* (1999). In the study by Fiala *et al.* (1999), the heat transfer coefficient is defined allowing for the heat transfer with insensible water loss. Insensible water loss is not proportional to the difference between body surface temperature and air temperature, as shown by Equation (3), and therefore should not be represented in the same manner for wide temperature variations. Thus, the equivalent heat transfer coefficient due to insensible water loss was calculated at 28°C. For P_{ins1} as in Table 3, the heat transfer coefficient between the skin and air in the adult female was calculated as 1.7 W/m^2/°C. The heat transfer coefficient from the skin to the air, including the insensible heat loss, was obtained as 5.7 W/m^2/°C. However, the numeric phantom used in the present study is descretized by voxels, and thus the surface of the phantom is approximately 1.4 times larger than that of an actual human (Samaras *et al.* 2006). Considering this difference, the actual heat transfer coefficient with insensible water loss is 7.8 W/m^2/°C, which is well within the uncertain range reported by Fiala *et al*. (1999).

In the next section, we consider the room temperature of 38°C, in addition to 28°C, in order to allow comparison with the temperatures measured by Tsuzuki et al. (1998). The insensible water loss is assumed to be the same as that at 28°C (Karshlake 1972). The heat transfer coefficient from the skin and air is chosen as 1.4 W/m^2/°C (Fiala *et al*. 1999). Since the air velocity in the lung would be the range of 0.5 and 1.0 m/s, the heat transfer coefficient H_2 can be estimated as 5 – 10 W/m^2/°C (Fiala *et al*. 1999). However, this uncertainty does not influence the computational results in the following discussion, because the difference between the internal air temperature and the body-core temperature is at most a few degrees, resulting in a marginal contribution to heat transfer (see Eq. (3)).

2. 4. Thermoregulatory Response in Adult and Child

For a temperature elevation above a certain level, the blood perfusion rate was increased in order to carry away excess heat that was produced. The variation of the blood perfusion rate in the skin through vasodilatation is expressed in terms of the temperature elevation in the hypothalamus and the average temperature increase in the skin. The phantom we used in the present study is the same as that used in our previous study (Hirata *et al*. 2007b). The variation of the blood perfusion rate in all tissues except for skin is marginal. This is because the threshold for activating blood perfusion is generally 2°C, while the temperature elevation of interest in the present study is at most 1°C, which is the rationale for human protection from RF exposure (ICNIRP, 1998).

Perspiration for the adult is modeled based on formulas presented by Fiala *et al*. (2001). The perspiration coefficients are assumed to depend on the temperature elevation in the skin and/or hypothalamus. An appropriate choice of coefficients could enable us to discuss the uncertainty

in the temperature elevation attributed to individual differences in sweat gland development:

$$SW(\mathbf{r},t) = \{W_S(\mathbf{r},t)\Delta T_S(t) + W_H(\mathbf{r},t)(T_H(t) - T_{Ho})\} / S \times 2^{(T(\mathbf{r})-T_0(\mathbf{r}))/10} \quad (7)$$

$$W_s(\mathbf{r},t) = \alpha_{11} \tanh(\beta_{11} T_s(\mathbf{r},t) - T_{so}(\mathbf{r})) - \beta_{10}) + \alpha_{10} \quad (8)$$

$$W_H(\mathbf{r},t) = \alpha_{21} \tanh(\beta_{21} T_s(\mathbf{r},t) - T_{so}(\mathbf{r})) - \beta_{20}) + \alpha_{20} \quad (9)$$

where S is the surface area of the human body, and W_S and W_H are the weighting coefficients for perspiration rate associated with the temperature elevation in the skin and hypothalamus. Fiala *et al.* (2001) determined the coefficients of α and β for the average perspiration rate based on measurements by Stolowijk (1971). In addition to the set of coefficients in Fiala *et al*. (2001), we determined the coefficients for adults with higher and lower perspiration rates parametrically (Hirata *et al*. 2007b). In the present study, we used these sets of parameters.

Thermoregulation in children, on the other hand, has not yet been well clarified. In particular, perspiration in children remains unclear (Bar-Or 1980, Tsuzuki *et al*. 1995). Therefore, heat stroke and exhaustion in children remain topics of interest in pediatrics (McLaren *et al*. 2005). Tsuzuki *et al*. (1995) and Tsuzuki (1998) found greater water loss in children than in mothers when exposed to heat stress. Tsuzuki *et al*. (1995) attributed the difference in water loss to differences in maturity level in thermophysiology (See also McLaren *et al*. 2005). However, a straightforward comparison cannot be performed due to physical and physiological differences. A number of studies have examined physiological differences among adults, children, and infants (e.g., Fanaroff *et al*. 1972, Stulyok *et al*. 1973). The threshold temperature for activating perspiration in infants (younger than several weeks of age) is somewhat higher than that for adults (at most 0.3°C). On the other hand, the threshold temperature for activating perspiration in children has not yet been investigated. In the present study, we assume that the threshold temperature for activating perspiration is the same in children and adults. Then, we will discuss the applicability of the present thermal model of an adult to an 8-month-old child by comparing the computed temperature elevations of the present study with those measured by Tsuzuki (1998).

3. Computational Results and Discussion

3. 1. Temperature Variation in the Adult and Child Exposed to Hot Room

3. 1.1. Computational Results for Temperature Variation in Adult

Our computational result will be compared with those measured by Tsuzuki (1998). The scenario in Tsuzuki (1998) was as follows: 1) resting in a thermoneutral room with temperature of 28°C and a relative humidity of 50%, 2) exposed to a hot room with temperature of 35°C and a relative humidity of 70% for 30 min., and 3) resting in a themoneutral room.

First, the perspiration model of Eq. (7) with the standard perspiration rate defined in Hirata *et al*. (2007b) is used as a fundamental discussion. Figures 2 and 3 show the time course of the

average skin and body-core temperature elevations, respectively, in the adult exposed to a hot room, together with those for an 8-month-old child. As shown in Fig. 2, the computed average temperature elevation of the adult skin was 1.5°C for a heat exposure time of 30 min., which is in excellent agreement with the measured data of 1.5°C. From Fig. 3, the measured and computed body-core temperatures in the adult female were 0.16°C and 0.19°C, respectively, which are well within the standard deviation of 0.05°C obtained in the measurement (Tsuzuki 1998). In this exposure scenario, the total water loss for an adult was 50 g/m^2 in our computation, whereas it was 60 g/m^2 in the measurements.

In order to discuss the uncertainty of temperature elevation due to the perspiration, the temperature elevations in the adult female is calculated for different perspiration parameters given in Hirata *et al*. (2007b). From Table 4(a), the set of standard perspiration parameters works better than other sets for determining the skin temperature. However, the body-core temperature for the standard perspiration rate was larger than that measured by Tsuzuki (1998). This is thought to be caused by the decrease in body-core temperature before heat exposure (0-10 min. in Fig. 3).

3.1.2. Computational Results for Temperature Variation in Child

Since thermal physiology in children has not been sufficiently clarified, we adapted the thermal model of the adult to the 8-month-old child for the fundamental discussion. The time courses of the average skin and body-core temperature elevations in the 8-month-old child are shown in Figs. 2 and 3, respectively. As shown in Fig. 2, the computed average temperature elevation of the skin of a child at 30 min. of heat exposure was 1.5°C, which is the same as that for an adult as well as the measured data. The measured and computed body-core temperatures in the child were 0.37°C and 0.41°C, respectively. This difference of 0.04°C is well within the standard deviation of 0.1°C obtained in the measurement (Tsuzuki 1998). In our computation, the total perspiration of the child was 100 g/m^2, whereas in the measurements, the value was 120 g/m^2; the same tendency was observed for the adult.

Table 4(b) lists the temperature elevations in the 8-month-old child for different perspiration parameters which were the same as we did for the adult. As with the adult, the model with the standard perspiration rate works better than the other models.

3.1.3. Discussion on the Thermal Model of the Adult and Child

From Fig. 2, an abrupt temperature decrease in the recovery phase after exposure in a hot room is observed in the measured data but is not observed in the computed data. The reason for this difference is discussed by Tsuzuki (1998), who reported that wet skin is suddenly cooled in a thermoneutral room. This phenomenon cannot be taken into account in our computational

modeling or boundary condition (Eqs. (3) and (4)). Such phenomenon would be considered with other boundary conditions, e.g., a formula by Ibrahiem et al (2005). However, this is beyond the scope of the present study, since our concern is on the temperature elevation in the body.

As shown by Fig. 3, the computed body-core temperature increases more quickly than the measured temperature. The time at which the body-core temperature became maximal in the measurement was retarded by 11 min. for the adult female whereas 5 min. for the child. There are two main reasons for this retard. One is caused by our assumption that the blood temperature is spatially constant and varies instantaneously (See Eq. (5)) based on the fact that the blood circulates throughout the body in 1 min. The other reason is that, in the experiment, we consider the blood temperature elevation instead of that in the rectum. The blood temperature in the rectum increases primarily due to blood circulation at an elevated temperature. In Hirata *et al*. (2007b), the temperature elevation in the hypothalamus, which is located in the brain and considerable as body core, was shown to be retarded by a few minutes relative to the blood temperature elevation. The difference of the retard between the adult and the child is attributed to the smaller body dimensions and greater blood perfusion rate of the child compared to those of the adult. The assumption in Eq. (5) was validated for rabbits (Hirata et al 2006b), the body dimensions of which are much smaller than those of a human. In addition, the blood perfusion rate of the rabbit is four times greater than that of the human adult, considering the difference in basal metabolic rate (Gordon *et al*. 1976). From this aspect, the thermal computational model used in this study works better for the child than for the adult. This retard in the body-core temperature elevation would give a conservative estimation from the standpoint of thermal dosimetry. In the following discussion, we consider not the temperature elevations at a specific time, but rather the peak temperatures for the measured data.

From table 4, we found some difference in total water loss between adult and child. One of the main reasons for this difference is thought to be the difference in race. The volunteers in the study by Tsuzuki (1998) were Japanese, whereas the data used for the computational modeling was based primarily on American individuals (Stolowijk, 1971). Roberts *et al*. (1970) reported that the number of active sweat glands in Korean individuals (similar to Japanese) is 20-30% greater than that in European individuals (similar to American). In addition, the perspiration rate in Japanese individuals is thought to be greater than that in American individuals, which was used to derive the perspiration formula.

Even though we applied a linear scaling when developing the 8-month-old child phantom, its influence on the temperature looks marginal. This is because the body-temperature is mainly determined by the heat balance between the energy produced through metabolic processes, energy exchange with the convection, and the energy storage in the body (Adair and Black 2003, Ebert et al 2005, Hirata et al 2008). Especially, the anatomy of the phantom does not influence

from the heat balance equation in the previous studies, suggesting that our approximation of the linear scaling was reasonable.

Tsuzuki et al. (1995) expected a maturity-related difference in themoregulatory response, especially for perspiration, between the adult and the child. The present study revealed two key findings. The first is the difference in the insensible water loss, which was not considered by Tsuzuki et al (1995). The other is the nonlinear perspiration response controlled by the temperature elevations in the skin and body core (Eq. (7)). In addition to these physiological differences, the larger body surface area-to-mass ratio generated more sweat in the child. The computational results of the present study considering these factors are conclusive and are consistent with the measured results.

From the discussion above, the validity of the thermal model for the adult was confirmed. In addition, the thermal model for the 8-month-old child is found to be reasonably the same as that of the adult.

3.2. Body-core Temperature Elevation in the Child and the Adult for Whole-body Exposures

3.2.1. Computational Results for Temperature Elevation duet to RF Exposures

An anatomically based human phantom is located in free space. As a wave source, a vertically polarized plane wave was considered; the plane wave was thus incident to a human phantom from the front. Female adult and 3-year-old child phantoms are considered in this section. The reason for using the 3-year-old child phantom is that this phantom is more anatomically correct than the 8-month-old child phantom, which was developed for comparison purposes in Section 3.1 simply by reducing the adult phantom.

The whole-body-averaged SAR has two peaks for plane-wave exposure at the ICNIRP reference level; more precisely, it becomes maximal at 70 MHz and 2 GHz in the adult female phantom and 130 MHz and 2 GHz in the 3-year-old child phantom. The first peak is caused by whole-body resonance in the human body. The latter peak, on the other hand, is caused by the relaxation of the ICNIRP reference level with the increase in frequency. Note that the power density at the ICNIRP reference level is 2 W/m^2 at 70 MHz and 130 MHz and 10 W/m^2 at 2 GHz. The whole-body-averaged SAR in the adult female phantom was 0.069 W/kg at 70 MHz and 0.077 W/kg at 2 GHz, whereas that in the 3-year-old child phantom was 0.084 W/kg at 130 MHz and 0.108 W/kg at 2 GHz. The uncertainty of whole-body SAR, attributed to the boundary conditions and phantom variability, has been discussed elsewhere (e.g., Findlay and Dimbylow 2006, Wang *et al*. 2006, Conil *et al*. 2008). In order to clarify the effect of frequency or the SAR distribution on the body-core temperature, we normalized the whole-body-averaged SAR as 0.08 W/kg while maintaining the SAR distribution. The normalized SAR distributions at these frequencies are illustrated in Fig. 4. As this figure shows, the SAR distributions at these

frequencies are quite different (Hirata *et al.* 2007a). EM absorption occurs over the whole body at the resonance frequency. Compared with the distribution at 2 GHz, the absorption around the body core cannot be neglected. In contrast, the SAR distribution is concentrated around the body surface at 2 GHz.

The temperature elevation distributions in a human are illustrated in Fig. 5 for the whole-body-averaged SAR of 0.08 W/kg. The duration of exposure was chosen as 60 min. As shown in Fig. 5, the SAR and temperature elevation distributions are similar. For example, the temperature elevation at the surface becomes larger at 2 GHz. However, the temperature in the body core (e.g., in the brain) is uniform at approximately 0.03°C. This is because the body core is heated mainly due to the circulation of warmed blood (Hirata *et al*. 2007b).

Figure 6 shows the time courses of the temperature elevation in the adult and the child at a whole-body-averaged SAR of 0.08 W/kg. This figure indicates that it took 4 hours to reach the thermally steady state. At 4 hours, the body-core temperature increases by 0.045°C at 65 MHz and 0.041°C at 2 GHz. This confirms the finding in our previous study (Hirata *et al*. 2007b) that whole-body-averaged SAR influences the body-core temperature elevation regardless of the frequency or SAR distribution. On the other hand, the temperature elevation in the child was 0.031°C at 130 MHz and 0.029°C at 2 GHz, which was 35% smaller than that in the adult.

Figure 7 shows the relationship between the whole-body-averaged SAR and the body-core temperature elevation when exposed for 1 hour. This duration was chosen so as to be longer than that considered in the ICNIPR guidelines (30 min.) and the thermal time constant for the male with a smaller perspiration rate (52 min.) in our previous study (Hirata *et al*. 2007b). In addition, the effect of frequency on the body-core temperature elevation is marginal for the whole-body-averaged SAR, as described in the above discussion. Therefore, only the relationship at whole-body resonance frequencies is given in this figure. The whole-body-averaged SAR required for a blood temperature increase of 1°C was 6.0 W/kg in the adult female phantom, whereas that in the 3-year-old child phantom was 9.0 W/kg. Note that the value of the adult female is comparable to 6.3 W/kg for NORMAN (a standard adult male phantom; Dimbylow 1997) in our previous study (Hirata *et al*. 2007b).

3.2.2 Discussion on the Difference of the Temperature Elevation between Adult and Child

We found significant difference of body-core temperature elevation between adult and child. We observed the reason for this difference as the difference in the body surface area-to-weight ratio. The total power deposited in the human is proportional to weight, as we fixed the whole-body-averaged SAR as 0.08 W/kg. On the other hand, the power loss from the human via perspiration is proportional to the surface area, because perspiration of the child can be considered as identical to that of the adult. As listed in Table 1, the ratio of the surface to the

weight is 0.029 m^2/kg for the adult, whereas that of the child is 0.043 m^2/kg. This difference of 47% coincides reasonably with the fact that body-core temperature elevation in the child is 35% smaller than that in the adult. Marginal inconsistency in these ratios would be caused by the nonlinear response of the perspiration as given by Eq. (7). For higher whole-body-averaged SAR, the ratio of temperature elevations in the adult to that of the child was 42%, which was closer to their body surface area-to-weight ratio of 47% than that in the case for the whole-body-averaged SAR at 0.08 W/kg. For higher temperature elevation, the effect of body-core temperature elevation on the perspiration rate is much larger than that due to skin temperature elevation. In addition, the perspiration rate becomes almost saturated. Therefore, the thermal response is considered to be linear with respect to the body-core temperature increase.

It is worth commenting on the difference between this scenario and that described in Section 3.1. In Section 3.1, the body-core temperature elevation in the child was larger than that in the adult for the heat stress caused by higher ambient temperature. The thermal energy applied to the body via ambient temperature is proportional to the surface area of the body. On the other hand, in this scenario, the thermal energy moves from the surface area of the body to the air, because the body is cooled via the ambient temperature. For these two cases, the main factor varying the body-core temperature is the same as the body surface area-to-weight ratio. However, the magnitude relation between the body surface and the ambient temperatures was reversed.

5. Conclusion

The temperature elevations in the anatomically based human phantoms of the adult and the 3-year-old child were calculated for radio-frequency (RF) whole-body exposure. The rationale for this investigation was that further research on the thermal dosimetry of children with appropriate thermoregulatory response is a high priority area in the RF research agenda proposed by the WHO (2006). However, systemic work on the difference in thermoregulation between young children and adults has not yet been performed, primarily because of ethical reasons and the lack of a reliable thermal computational model. In the present study, we discussed a computational thermal model of a child for simulating body-core temperature elevation in child phantoms by comparing the experimental results of volunteers when exposed to a high ambient temperature. The computational results revealed the thermal response in the 8-month-old child to be approximately the same as that in the adult. Based on this finding, we calculated the body-core temperature elevation in the 3-year-old child and the adult for plane wave exposure at the ICNIRP basic restriction. The body-core temperature elevation in the 3-year-old child phantom was 40% smaller than that in the adult phantom, which is attributed to

the difference in the ratio of the body surface area to the mass between the child and the adult. The whole-body-averaged SAR required for a blood temperature increase of 1°C was 9.0 W/kg in the 3-year-old child phantom, whereas that was in the adult female phantom was 6.0 W/kg.

Acknowledgements

The authors would like to acknowledge Drs. Soichi Watanabe and Tomoaki Nagaoka for providing their anatomically based Japanese phantoms. The present study was supported in part by the Ministry of Education, Science, Sports, and Culture through a Grant-in-Aid for Scientific Research (B), and by the International Communications Foundation of Japan.

REFERENCES

Adair E. R., Kelleher S. A., Mack G. W., and Morocco T. S. 1998 Thermophysiological responses of human volunteers during controlled whole-body radio frequency exposure at 450 MHz Bioelectromagnetics **19** 232-245

Adair E. R., Cobb B. L., Mylacraine K. S., Kelleher S. A. 1999 Human exposure at two radio frequencies (450 and 2450 MHz): Similarities and differences in physiological response Bioelectromagnetics **20** (suppl 4) 12-20

American Conference of Government Industrial Hygienists (ACGIH) 1996 Threshold limit values for chemical substances and physical agents and biological exposure indices (Cincinnati OH)

Bernardi P, Cavagnaro M, Pisa S and Piuzzi E 2003 Specific absorption rate and temperature elevation in a subject exposed in the far-field of radio-frequency sources operating in the 10-900-MHz range *IEEE Trans. Biomed. Eng*. **50** 295-304

Conil E, Hadjem A, Lacroux, Wong M F and Wiart J 2008 Variability analysis of SAR from 20 MHz to 2.4 GHz for different adult and child models using finite-difference time-domain *Phys. Med. Biol.* **53** 1511-1525

Cooper T E and Trezek G J 1971 Correlation of thermal properties of some human tissue with water content *Aerospace Med.* **50** 24-27

Chatterjee I and Gandhi O P 1983 An inhomogeneous thermal block model of man for the electromagnetic environment *IEEE Trans. Biomed. Eng.* **30** 707-715

Dimbylow P J 1997. FDTD calculations of the whole-body averaged SAR in an anatomically realistic voxel model of the human body from 1 MHz to 1 GHz. Phys. Med. Biol. **42** 479-90

Dimbylow P J 2002 Fine resolution calculations of SAR in the human body for frequencies up to 3 GHz *Phys. Med. Biol.* **47** 2835-2846

Douglas H K 1977 Handbook of Physiology, Sec. 9, Reactions to environmental agents

MD:American Physiological Society

Ebert S, Eom S J, Schuderer J, Spostel U, Tillmann T, Dasenbrock C, and Kuster N. 2005 Response, thermal regulatory threshold of restrained RF-exposed mice at 905 MHz. Phys Med Biol **50** 5203-5215

Fanaroff A A, Wald M, Gruber H S, Klaus M H 1972 Insensible water loss in low birth weight infants *Pediatrics* **50** 236-245

Fiala D, Lomas K J and Stohrer M 1999 A computer model of human thermoregulation for a wide range of environmental conditions: the passive system *J Appl Physiol* **87** 1957-1972

Fiala D, Lomas K J and Stohrer M 2001 Computer prediction of human thermoregulation and temperature responses to a wide range of environmental conditions *Int J Biometeorol* **45** 143-159

Findlay R P and Dimbylow P J 2006 Variations in calculated SAR with distance to the perfectly matched layer boundary for a human voxel model *Phys. Med. Biol.* **51** N411-N415

Follow B and Neil E Eds 1971 Circulation, Oxford Univ. Press (New York USA)

Foster K R and Adair E R 2004 Modeling thermal responses in human subjects following extended exposure to radiofrequency energy *Biomed. Eng. Online* 3:4

Fujimoto S, Watanabe T, Sakamoto A, Yukawa K, and Morimoto K 1968. Studies on the physical surface area of Japanese. 18. Calculation formulas in three stages over all ages. Nippon Eiseigaku Zasshi 23: 443-450 (in Japanese).

Gabriel C 1996 Compilation of the dielectric properties of body tissues at RF and microwave frequencies. Final Tech Rep Occupational and Environmental Health Directorate. AL/OE-TR-1996-0037 (Brooks Air Force Base, TX: RFR Division)

Gordon RG, Roemer R B and Horvath S M 1976 A mathematical model of the human temperature regulatory system-transient cold exposure response *IEEE Trans Biomed Eng* **23** 434-444

Hardy J D and DuBois E F 1938 Basal metabolism, radiation, convection, and vaporization at temperatures of 22-35 ^{o}C *J. Nutr.* **15** 477

Hirata A, Fujiwara O and Shiozawa T 2006a Correlation between peak spatial-average SAR and temperature increase due to antennas attached to human trunk *IEEE Trans. Biomed. Eng.* **53** 1658-64

Hirata A, Watanabe S, Kojima M, Hata I, Wake K, Taki M, Sasaki K, Fujiwara O and Shiozawa T 2006b Computational verification of anesthesia effect on temperature variations in rabbit eyes exposed to 2.45-GHz microwave energy *Bioelectromagnetics* **27** 602-612

Hirata A, Kodera S, Wang J and Fujiwara O 2007a Dominant factors influencing whole-body average SAR due to far-field exposure in whole-body resonance frequency and GHz regions *Bioelectromagnetics* **28** 484-487

Hirata A, Asano T, and Fujiwara O 2007b FDTD analysis of human body-core temperature elevation due to RF far-field energy prescribed in ICNIRP guidelines *Phys Med Biol* **52**

5013-5023

Hirata A, Sugiyama H, Kojima M, Kawai H, Yamashiro Y, Fujiwara O, Watanabe S, and Sasaki K 2008 Computational model for calculating body-core temperature elevation in rabbits due to whole-body exposure at 2.45 GHz Phys. Med. Biol.

Hoque M and Gandhi O P 1988 Temperature distribution in the human leg for VLF-VHF exposure at the ANSI recommended safety levels *IEEE Trans. Biomed. Eng.* **35** 442-449.

Ibrahiem A, Dale C, Tabbara W, Wiart J 2005 Analysis of the Temperature Increase Linked to Power Induced by RF Source Progress in Electromagnet. Res **52** 23-46.

International Commission on Radiological Protection (ICRP) 1975 Report of the Task Group on Reference Man vol.23, Pergamon Press:Oxford.

International Commission on Non-Ionizing Radiation Protection (ICNIRP) 1998 Guidelines for limiting exposure to time-varying electric, magnetic, and electromagnetic fields (up to 300 GHz)., *Health Phys.* **74** 494-522

Karslake D. De. K 1972 The stress of hot environment. Cambridge Univ. Press, London.

Kotte A, vanLeeuwen G, deBree J, vanderKoijk J, Crezee H and Lagendijk J 1996 A description of discrete vessel segments in thermal modeling of tissues *Phys. Med. Biol.* **41** 865-884

Margaret W, Johnston W, and Newburgh L H 1942 Calculation of heat production from insensible loss of weight *J Clin Invest.* **21** 357–363

McLaren C, Null J, and Quinn J 2005 Heat stress from enclosed vehicles: moderate ambient temperatures cause significant temperature rise in enclosed vehicles **116** e109-e112

Nagaoka T, Watanabe S, Sakurai K, Kunieda E, Watanabe S, Taki M and Yamanaka Y 2004 Development of realistic high-resolution whole-body voxel models of Japanese adult males and females of average height and weight, and application of models to radio-frequency electromagnetic-field dosimetry *Phys. Med. Biol.* 49 1-15

Nagaoka T, Horise S, Fukuda K, Kunieda E, Wang J, Fujiwara O and Watanabe S 2005 Development of the child voxel models by transforming the adult voxel model *IEICE Tech. Rep.* EMCJ2005-26, 2005.

Nakayama T and Iriki M Ed. 1987 Handbook of Physiological Science vol.18: Physiology of Energy Exchange and Thermoregulation Igaku-Shoin (Tokyo)

Bar-Or O 1994 Dotan R, Inbar O, Rotshtein A and Zonder H 1980 Voluntary hypohydration in 10 to 12 year old boys J. Appl. Physiol. **48** 104-108.

Pennes H H 1948 Analysis of tissue and arterial blood temperatures in resting forearm *J. Appl. Physiol.* **1** 93-122

Roberts D.F., Salzano F M, and Willson J. O. C. 1970 Active sweat gland distribution in caingang Indians *Am. J. Phys. Anthrop.* **32** 395-400

Samaras T, Christ A, and Kuster N 2006 Effects of geometry discretization aspects on the numerical solution of the bioheat transfer equation with the FDTD technique *Phys. Med.*

Biol. **51** 221-229

Spiegel R J 1984 A review of numerical models for predicting the energy deposition and resultant thermal response of humans exposed to electromagnetic fields *IEEE Trans. Microwave Theory Tech.* **32** 730-746

Stolwijk J A J 1971 A mathematical model of physiological temperature regulation in man. Washington, DC: NASA (CR-1855)

Stulyok E, Jequier E, and Prodhom L S 1973 Respiratory contribution to the thermal balance of the newborn infant under various ambient conditions *Pediatrics* **51** 641-50

Taflove A and Hagness S 2003 Computational Electrodynamics: The Finite-Difference Time-Domain Method: 3rd Ed. Norwood. MA: Artech House

Tsuzuki K, Tochibara Y, and Ohnaka T 1995 Thermoregulation during heat exposure of young children compared to their mothers *Eur. J. Appl. Physiol.* **72** 12-17

Tsuzuki K 1998 Thermoregulation during hot and warm exposures of infants compared to their mothers Jpn. Soc. Home Economics **49** 409-415

Wang J, Kodera S, Fujiwara O and Watanabe S 2005 FDTD calculation of whole-body average SAR in adult and child models for frequencies from 30 MHz to 3 GHz *Phys Med Biol* **51** 4119-4127

FIGURE AND TABLE CAPTIONS

Figure 1. Anatomically based human body phantoms of (a) a female adult, (b) a 3-year-old child, and (c) an 8-month-old child.

Figure 2. Time course of average skin temperature elevations in the adult and the 8-month-old child.

Figure 3. Time course of body-core temperature elevations in the adult and the 8-month-old child.

Figure 4. SAR distributions in the adult female at (a) 70 MHz and (b) 2 GHz and those in the 3-year-old child model at (c) 130 MHz and (d) 2 GHz.

Figure 5. Temperature elevation distributions in the adult female at (a) 70 MHz and (b) 2 GHz and those in 3-year-old child model at (c) 130 MHz and (d) 2 GHz.

Figure 6. Temperature elevation in the adult and 3-year-old child at the whole-body-averaged SAR of 0.08 W/kg. The duration of exposure was 4 hours.

Figure 7. Dependency of body-core temperature elevation on whole-body-averaged SAR. The duration of exposure was 60 min.

Table 1. Height, weight, and surface area of Japanese phantoms.

Table 2. Thermal constants of adult tissues.

Table 3. Insensible water loss and heat transfer rate in the adult female and 3-year-old and 8-month-old children.

Table 1

	H [m]	W [kg]	S [m^2]	S/W [m^2/kg]
Female	1.61	53	1.5	0.029
3 year old	0.90	13	0.56	0.043
8 month old	0.75	9	0.43	0.047

Table 2

tissue	K[W m^{-1} ^oC]	C[J kg^{-1} ^oC]	ρ[kg m^{-3}]	B[W m^{-3} ^oC]	A[W m^{-3}]
air	0	0	0	0	0
Internal air	0	0	0	0	0
skin	0.27	3600	1125	1700	1620
muscle	0.40	3800	1047	2000	480
fat	0.22	3000	500	1500	300
bone (cortical)	0.37	3100	1990	3400	610
bone (cancellous)	0.41	3200	1920	3300	590
nerve (spine)	0.46	3400	1038	40000	7100
gray matter	0.57	3800	1038	40000	7100
CSF	0.62	4000	1007	0	0
eye (aqueous humor)	0.58	4000	1009	0	0
eye (lens)	0.40	3600	1053	0	0
eye (sclera/wall)	0.58	3800	1026	75000	22000
heart	0.54	3900	1030	54000	9600
liver	0.51	3700	1030	68000	12000
lung (outer)	0.14	3800	1050	9500	1700
kidneys	0.54	4000	1050	270000	48000
intestine (small)	0.57	4000	1043	71000	13000
intestine (large)	0.56	3700	1043	53000	9500
gall bladder	0.47	3900	1030	9000	1600
spleen	0.54	3900	1054	82000	15000
stomach	0.53	4000	1050	29000	5200
pancreas	0.52	4000	1045	41000	7300
blood	0.56	3900	1058	0	0
body fluid	0.56	3900	1010	0	0
bile	0.55	4100	1010	0	0
glands	0.53	3500	1050	360000	64000
bladder	0.43	3200	1030	9000	160
testicles	0.56	3900	1044	360000	64000
lunch	0.56	3900	1058	0	0
adrenals	0.42	3300	1050	270000	48000
Tendon	0.41	3300	1040	9000	1600

Table 3

	P_{ins1}[W]	P_{ins2}[W]	H_1[W m^{-2} ^{o}C]	H_2[W m^{-2} ^{o}C]
Female	20.3	8.7	4.1	26.0
3 year old	10.7	4.6	4.0	13.1
8 month old	8.9	3.8	3.9	13.3

Table 4

(a)

child	low	standard	high	measured
skin	2.0	1.5	0.98	1.5
body-core	0.50	0.41	0.32	0.37

(b)

adult	low	standard	high	measured
skin	1.7	1.5	1.2	1.5
body-core	0.21	0.19	0.17	0.16

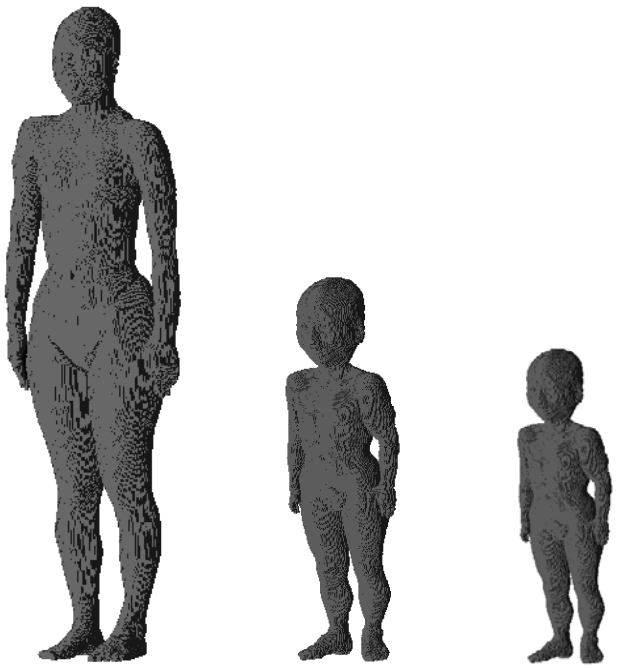

Figure 1

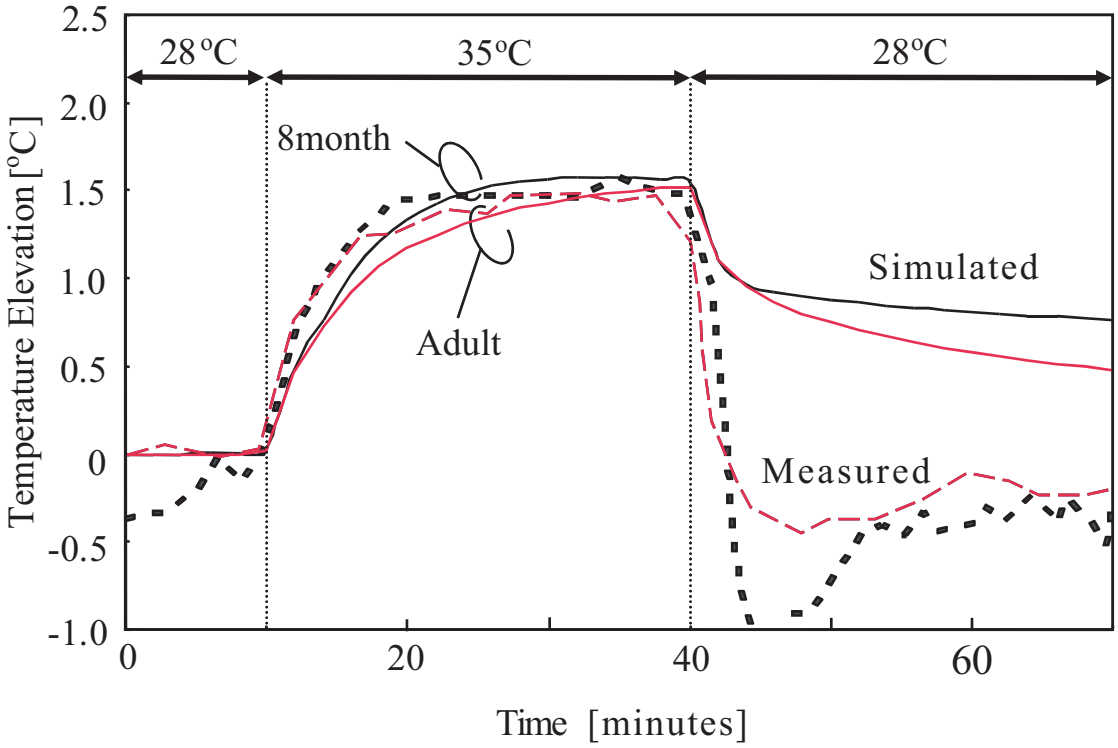

Figure 2

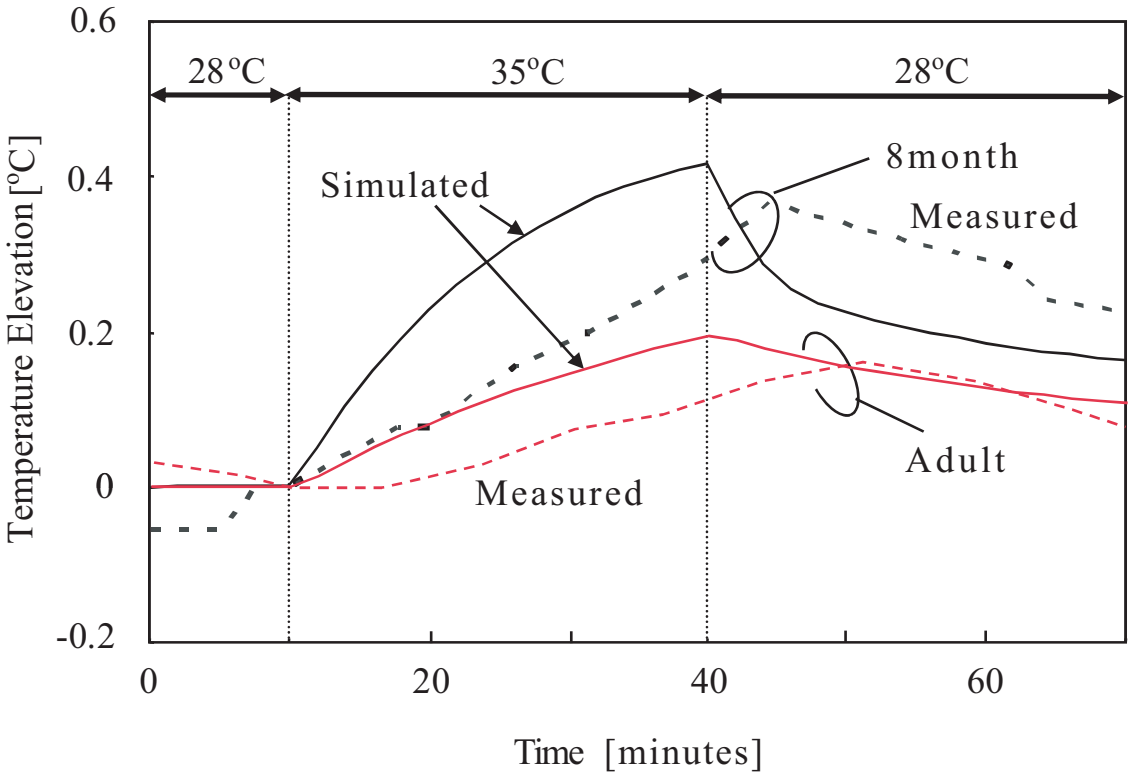
0.6
0.4
0.2
0
-0.2
Temperature Elevation [°C]
28°C
35°C
28°C
Simulated
8month
Measured
Adult
Measured
0
20
40
60
Time [minutes]

Figure 3

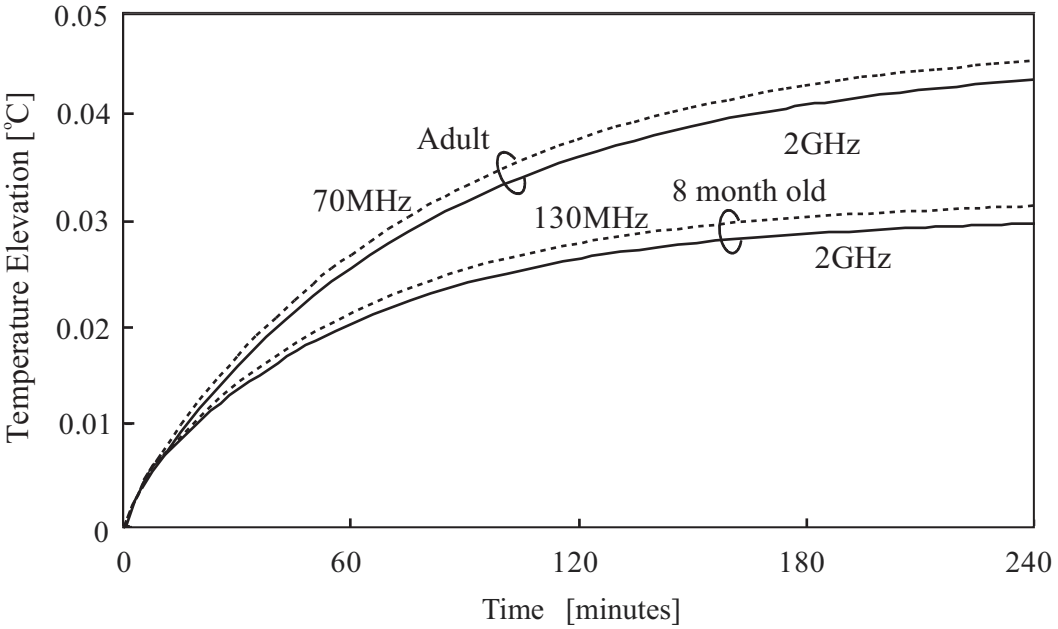

Figure 6

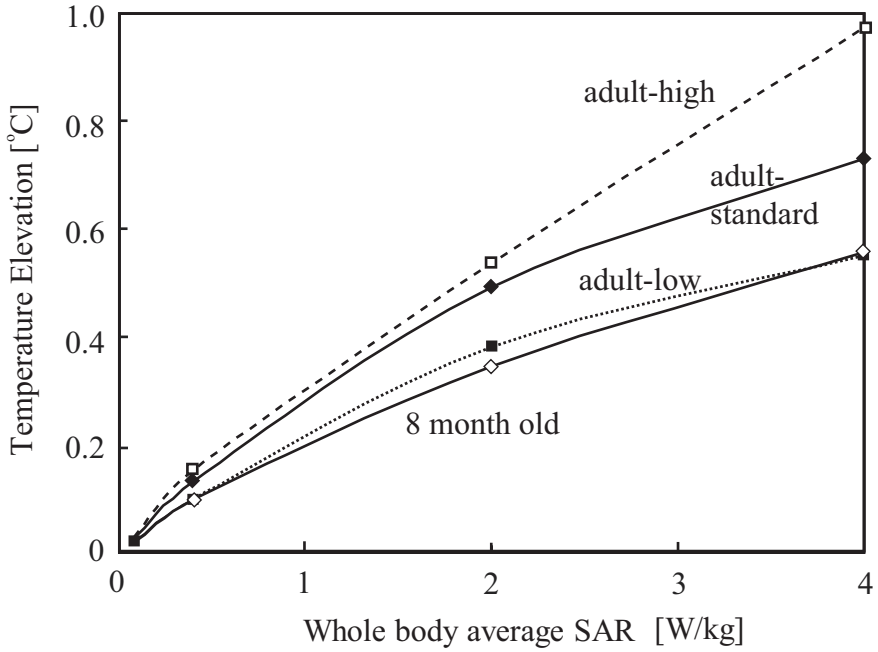

Figure 7